NIH Public Access
Author Manuscript
Cell. Author manuscript; available in PMC 2009 May 2.

Published in final edited form as:
Cell. 2008 May 2; 133(3): 475–485. doi:10.1016/j.cell.2008.02.053.

Pirt, a Phosphoinositide-Binding Protein, Functions as a Regulatory Subunit of TRPV1

Andrew Y. Kim[1,2], **Zongxiang Tang**[1,2], **Qin Liu**[1], **Kush N. Patel**[1], **David Maag**[1], **Yixun Geng**[1], and **Xinzhong Dong**[1,*]

1*The Solomon H. Snyder Department of Neuroscience, Center for Sensory Biology, School of Medicine, Johns Hopkins University, Baltimore, MD 21205, USA*

Abstract

SUMMARY—Transient receptor potential vanilloid 1 (TRPV1) is a molecular sensor of noxious heat and capsaicin. Its channel activity can be modulated by several mechanisms. Here we identify a membrane protein, Pirt, as a regulator of TRPV1. Pirt is expressed in most nociceptive neurons in the dorsal root ganglia (DRG) including TRPV1-positive cells. Pirt null mice show impaired responsiveness to noxious heat and capsaicin. Noxious heat- and capsaicin-sensitive currents in Pirt-deficient DRG neurons are significantly attenuated. Heterologous expression of Pirt strongly enhances TRPV1-mediated currents. Furthermore, the C terminus of Pirt binds to TRPV1 and several phosphoinositides, including phosphatidylinositol-4,5-bisphosphate (PIP_2), and can potentiate TRPV1. The PIP_2 binding is dependent on the cluster of basic residues in the Pirt C terminus and is crucial for Pirt regulation of TRPV1. Importantly, the enhancement of TRPV1 by PIP_2 requires Pirt. Therefore, Pirt is a key component of the TRPV1 complex and positively regulates TRPV1 activity.

INTRODUCTION

In mammals, pain sensation or nociception is initiated by a subset of sensory neurons, known as nociceptive neurons, in the dorsal root ganglia (DRG) (Scott, 1992). The essential functions of nociceptive neurons are detecting noxious thermal, mechanical, and chemical stimuli in the environment, converting them to electrochemical signals, and sending signals to the spinal cord. Nociceptive neurons can also become sensitized after tissue injury or inflammation such that innocuous stimuli can activate them (Scott, 1992).

In recent years, the family of transient receptor potential (TRP) channels has attracted interest due to its importance in various sensory systems including thermosensation and nociception (Montell, 2005). TRPV1, a nonselective cation channel of six transmembrane domains, was identified by its responsiveness to noxious heat (>43°C) and capsaicin from chili peppers (Caterina et al., 1997; Tominaga et al., 1998). TRPV1 is expressed primarily in small-to-medium diameter nociceptive neurons. *TRPV1*$^{-/-}$ mice show a complete absence of behavioral responses to capsaicin and impaired responses to painful heat (Caterina et al., 2000). In addition, cultured sensory neurons from *TRPV1*$^{-/-}$ mice show a loss of capsaicin responses and thermal (42°C–52°C) sensitivity (Caterina et al., 2000; Davis et al., 2000). TRPV1 also

*Correspondence: xdong2@jhmi.edu.
[2]These authors contributed equally to this work.

ACCESSION NUMBERS
The GenBank Accession Number for Pirt is EU447173.

SUPPLEMENTAL DATA
Supplemental Data include seven figures and Supplemental Experimental Procedures and can be found with this article online at http://www.cell.com/cgi/content/full/133/3/475/DC1/.

NIH-PA Author Manuscript
NIH-PA Author Manuscript
NIH-PA Author Manuscript

NIH-PA Author Manuscript

NIH-PA Author Manuscript

NIH-PA Author Manuscript

plays a critical role in thermal inflammatory hyperalgesia since its activity can be potentiated by inflammatory mediators such as nerve growth factor and bradykinin (Chuang et al., 2001). These mediators act through various mechanisms, including phosphorylation of intracellular residues or increased membrane expression (Huang et al., 2006).

The activity of TRPV1 can also be modulated by phosphoinositides (PIPs). For example, TRPV1 can be negatively regulated by phosphatidylinositol-4,5-bisphosphate (PIP_2)(Chuang et al., 2001). A putative PIP_2-binding domain in the C terminus of TRPV1 has been identified, and mutations in this domain result in increased TRPV1 baseline currents and reduced thermal threshold and sensitivity to capsaicin (Prescott and Julius, 2003). However, recent studies have shown that PIP_2 can have an activating effect on TRPV1 (Liu et al., 2005). When PIP_2 (or other PIPs) is added heterologously to excised inside-out membrane patches, TRPV1-mediated current is enhanced (Stein et al., 2006; Lukacs et al., 2007). These data suggest that PIP_2 plays a dual role in TRPV1 regulation. More recently, it was shown that TRPV1 can directly bind PIPs and that this binding disrupts the association of calmodulin (CaM) with TRPV1 (Kwon et al., 2007).

Despite the clear physiological importance of TRPV1, little is known about TRPV1-associated proteins and the subunit structure of TRPV1 complexes. Here we describe a membrane protein, called *p*hosphoinositide *i*nteracting *r*egulator of *T*RP (Pirt), which is expressed specifically in the peripheral nervous system (PNS), predominantly in nociceptive neurons. *Pirt* null (*Pirt*$^{-/-}$) mice exhibit phenotypes that resemble those observed in *TRPV1*$^{-/-}$ mice, though they are less severe. *Pirt*-deficient DRG neurons have significantly lower noxious heat- and capsaicin-evoked currents than those observed in wild-type (WT) neurons. Consistently, coexpression of Pirt and TRPV1 in HEK293 cells significantly enhances TRPV1-mediated currents. Furthermore, the C terminus of Pirt binds TRPV1 and several PIPs including PIP_2 and is sufficient to potentiate TRPV1 activity. Lastly, we found that Pirt and PIP_2 require each other to enhance TRPV1. These data suggest that Pirt is a component of the TRPV1 complex and positively regulates the channel activity via PIP_2.

RESULTS

Identification of *Pirt*: A Gene Strongly Expressed in DRG but Not in the CNS

A cDNA subtractive screen using neonatal WT and *Ngn1*$^{-/-}$ mouse DRG was performed to find genes specifically expressed in nociceptive neurons (Dong et al., 2001). From this screen, we isolated a previously uncharacterized gene encoding a 135 amino acid membrane protein named Pirt based on its function. The predicted Pirt protein sequence is highly conserved among vertebrates (Figure 1A). Using the TMHMM program we predicted that Pirt has two transmembrane domains. It is likely that Pirt is inserted into the membrane as a hairpin with both N and C termini in the cytoplasm (Figure 1E). Pirt protein does not contain any known functional domains with the exception of clusters of positively charged residues, characteristic of PIP-binding motifs (Wang et al., 2001), at its C terminus (Figure 1A). In situ hybridization revealed that *Pirt* is strongly expressed in most DRG (Figures 1B and 1C) and trigeminal neurons (data not shown). Weaker staining was also found in other parts of the PNS including sympathetic (Figure 1D) and enteric (data not shown) neurons. Strikingly, there was no *Pirt* expression in the spinal cord (Figure 1B). *Pirt* is first expressed in DRG neurons around embryonic day 11.5, and expression is maintained throughout adulthood. Consistently, Pirt protein is specifically detected in the PNS (Figure S1 available online).

Generation of *Pirt*$^{-/-}$ Mice

To study Pirt function in vivo, we generated *Pirt* null (*Pirt*$^{-/-}$) mice. In these mice, the entire open reading frame of *Pirt* was replaced by the axonal tracer farnesylated enhanced green

NIH-PA Author Manuscript

NIH-PA Author Manuscript

NIH-PA Author Manuscript

fluorescent protein (EGFPf) (Figure 2A). Expression of the knockin EGFPf is under control of the endogenous *Pirt* promoter. The resulting $Pirt^{-/-}$ animals are viable, fertile, and indistinguishable from WT littermates in appearance. They show normal locomotion (Figure S4D) and overt behavior. Mating between heterozygous animals produced WT, heterozygous, and homozygous mutant offspring with expected Mendelian ratios. The deletion of Pirt protein in $Pirt^{-/-}$ mice was confirmed by western blot of DRG lysates using anti-Pirt antibody (Figure 2B). In contrast, TRPV1 protein levels of $Pirt^{+/+}$ and $Pirt^{-/-}$ DRG neurons are similar (Figure 2B). WT and $Pirt^{-/-}$ mice also have the same proportions of CGRP-, IB4-, and NF200-immunoreactive neurons (i.e., different subtypes of sensory neurons) to the total number of DRG neurons (Figure 2C). Furthermore, the percentages of $TRPV1^+$ neurons are comparable in WT and $Pirt^{-/-}$ mice (Figure 2C). The immunoreactivity and projection patterns of $TRPV1^+$, $CGRP^+$, and $IB4^+$ primary afferents to the spinal cord are similar between the two groups (Figure S2). These results suggest that Pirt is not involved in the development of nociceptive neurons.

Pirt Is Expressed by Most $CGRP^+$ and $IB4^+$ DRG Neurons

Since the expression of the knockin EGFPf is under control of the endogenous *Pirt* promoter, EGFPf should be expressed by $Pirt^+$ neurons in *Pirt-EGFPf* knockin mice. Anti-GFP antibody staining revealed that GFP is widely expressed in the DRG isolated from these mice, labeling 83.9% of all neurons. This staining pattern reflects the results from in situ hybridization using *Pirt* riboprobe. We then assessed whether *Pirt* is expressed by peptidergic ($CGRP^+$) and/or nonpeptidergic ($IB4^+$) neurons, two major subtypes of unmyelinated nociceptive C-fibers (Caterina and Julius, 1999). Double immunofluorescence staining revealed that most if not all $CGRP^+$ and $IB4^+$ neurons express *Pirt* (Figures S3A and S3B). Myelinated neurons, visualized by anti-neurofilament 200 (NF200) antibody, partially overlap with $Pirt^+$ neurons (Figure S3C). The *Pirt*-expressing myelinated neurons may include thinly myelinated nociceptive Aδ fibers and other myelinated non-nociceptive neurons. Importantly, subsets of $Pirt^+$ neurons express TRPV1 (Figure S3D). Most *Pirt*-negative neurons are $NF200^+$ and have large-diameter cell bodies (36.7 ± 1.8 mm). Furthermore the axons of Pirt-expressing neurons project to both laminae I and II of the dorsal spinal cord, the central projection sites for most nociceptive fibers (Figures S3E and S3F).

Pirt Null Mice Have Impaired Behavioral Responses to Noxious Heat and Capsaicin

Since *Pirt* is expressed in most C-fiber nociceptive neurons, we performed a battery of nociceptive behavioral experiments on $Pirt^{-/-}$ mice and WT littermates to assess the possible involvement of Pirt in nociception. To study the behavioral responses to noxious heat, we first performed the tail immersion test, where the latency time for the mice to withdraw their tails after tail immersion into heated water baths was recorded. $Pirt^{-/-}$ mice exhibited significantly prolonged tail-withdrawal latency at temperatures of 48°C, 50°C, and 52°C as compared to WT controls (Figure 3A). The tail-withdrawal latency at 46°C was not significantly different between the two groups (data not shown). We then performed the hot-plate assay (Figure 3B). Mice were placed on a hot surface and the latency time for shaking or licking of the hindpaw was measured. The $Pirt^{-/-}$ mice showed a significant increase in the latency time at temperatures of 50°C and 52.5°C. At 48°C (data not shown) and 55°C (Figure 3B), mutant mice still showed increased latency time compared to WT mice, but the difference was not significant. In the Hargreaves assay (radiant heat), a similar reduction in heat sensitivity was seen in *Pirt*-deficient animals (Figure S4A). Furthermore, thermal hyperalgesia (elevated pain sensitivity) under inflamma-tory conditions was reduced in the mutant mice (Figure S4). These results indicate that $Pirt^{-/-}$ mice have impaired behavioral responses to noxious heat.

In addition to thermosensation, we evaluated chemically and mechanically evoked pain responses in $Pirt^{-/-}$ mice. Intraplantar injection of capsaicin was performed on WT and

NIH-PA Author Manuscript

NIH-PA Author Manuscript

NIH-PA Author Manuscript

Pirt$^{-/-}$ mice. The time spent by the mice licking and biting of the hindpaw was recorded. A significant reduction in the response time was observed in *Pirt*$^{-/-}$ mice (15.7 ± 2.3 s) as compared to WT mice (24.2 ± 2.5 s) (Figure 3C). When sensitivity to acid was tested on the WT and *Pirt*$^{-/-}$ mice, the mutant mice showed a slight, but statistically insignificant, increase in sensitivity (Figure 3E). We also injected mustard oil into the mouse hindpaw and recorded time spent licking the affected paw, which is a behavior mediated by TRPA1 (Bautista et al., 2006; Kwan et al., 2006). WT and *Pirt*$^{-/-}$ mice showed similar responses in this test (Figure 3G). Licking behavior induced by intraplantar injection of formalin into the hindpaw was also similar between *Pirt*$^{-/-}$ and WT mice (Figure 3F). Furthermore, the two groups exhibited similar mechanical responses under normal or inflammatory conditions (Figures 3D and S4C). These results show that Pirt is required for capsaicin-induced pain behavior but not for other chemically or mechanically evoked responses.

TRPV1-Mediated Currents Are Attenuated in DRG Neurons Lacking Pirt

The behavioral phenotypes of *Pirt*$^{-/-}$ mice resemble those observed in *TRPV1*$^{-/-}$ mice (Caterina et al., 2000). We hypothesized that the altered mouse behavior could be attributed to defects in the ability of the TRPV1 channel to conduct current in the absence of Pirt. We tested this hypothesis by performing whole-cell patch clamp recordings on dissociated DRG neurons isolated from WT and *Pirt*$^{-/-}$ mice. Since TRPV1 is expressed in small- and medium-diameter nociceptive neurons (Caterina et al., 2000), we recorded DRG neurons with cell body diameters ranging from 18 μm to 25 μm (means at 21.4 μm for both genotypes). Inward currents generated by noxious heat were found in 53.0% of DRG neurons (n = 76) from *Pirt*$^{+/+}$ mice. A similar number of DRG cells (52.8%; n = 70) from *Pirt*$^{-/-}$ mice also responded to noxious heat, consistent with the fact that percentages of TRPV1-expressing cells are similar in WT and *Pirt*$^{-/-}$ mice (Figure 2C). Although the percentages of DRG neurons responding to noxious heat in these two genotypes are similar, the current sizes of responsive neurons from *Pirt*$^{-/-}$ mice are significantly smaller than those of WT mice (Figures 4A and 4B). The average currents in WT and *Pirt*$^{-/-}$ neurons were 3.0 ± 0.3 nA and 1.9 ± 0.2 nA, respectively (p = 0.008). When the average current size was divided by cell capacitance to normalize the current to cell size, the current over capacitance values were 94.8 ± 8.7 pA/pF and 56.6 ± 4.0 pA/pF for the WT and *Pirt*$^{-/-}$ neurons, respectively (p = 0.0002). The heat activation threshold was not significantly different between the two groups (WT: 43.2°C ± 0.8°C; *Pirt*$^{-/-}$: 44.7°C ± 0.7°C). These data show that the absence of Pirt reduces the ability of TRPV1 to conduct current in response to noxious temperatures.

We also examined capsaicin-evoked currents in *Pirt*$^{+/+}$ and *Pirt*$^{-/-}$ neurons. Again, the proportion of DRG neurons responding to capsaicin was the same in WT (56.0%; n = 294) and mutant (57.0%; n = 268) neurons. We applied different doses of capsaicin to dissociated neurons to determine TRPV1 sensitivity. Although *Pirt*$^{-/-}$ neurons exhibited less capsaicin-activated current than WT neurons at every concentration tested, statistically significant reductions were only found at higher capsaicin concentrations (5 and 10 μM; Figures 4C and 4D). The half-maximal effective doses (EC_{50}) for activating capsaicin-sensitive currents were similar between WT (0.99 ± 0.03 μM) and *Pirt*$^{-/-}$ (1.02 ± 0.07 μM) neurons, suggesting that Pirt affects the efficacy but not potency of capsaicin-induced current. These results are not due to a Pirt-dependent reduction in total expression of TRPV1 and TRPV1 membrane trafficking in DRG neurons (Figure 2B). These electrophysiological experiments demonstrate that Pirt is required for normal noxious heat- and capsaicin-evoked currents.

TRPV1 can be potentiated by bradykinin via both protein kinase C (PKC) and phospholipase C (PLC) dependent pathways (Hardie, 2007). *Pirt*$^{-/-}$ neurons exhibited a reduction in bradykinin-mediated TRPV1 potentiation (Figures 4E and 4F), suggesting that Pirt plays a role in this process (see Discussion).

NIH-PA Author Manuscript

NIH-PA Author Manuscript

NIH-PA Author Manuscript

We next addressed whether deletion of Pirt affects the function of other ion channels in nociceptive neurons. We found that *Pirt*$^{-/-}$ neurons respond normally to neurotransmitter γ-amino-butyric acid (GABA) (Figures S5A and S5B). Voltage-sensitive inward currents are similar between WT and *Pirt*$^{-/-}$ neurons (Figures S5C–S5E). Consistent with our behavioral data, *Pirt*$^{-/-}$ neurons responded normally to mustard oil (TRPA1 agonist) as assessed by calcium imaging (Figure S5H). These results suggest that although TRPV1-mediated currents are greatly reduced in *Pirt*$^{-/-}$ neurons, other ion channels function normally.

Pirt Enhances TRPV1 Activity

The *Pirt*$^{-/-}$ behavioral and cellular loss-of-function phenotypes strongly suggest that Pirt positively regulates TRPV1 channel activity. To further test this hypothesis, we examined whether Pirt itself has the ability to enhance TRPV1 activity in a heterologous system. We transfected Pirt cDNA into a HEK293 cell line that stably expresses TRPV1 (Guler et al., 2002) and measured currents in response to noxious temperatures in TRPV1- or TRPV1/Pirt-expressing cells. We used the TRPV1 stably expressing cell line instead of transient transfection of TRPV1 in order to keep the level of TRPV1 more consistent. When the temperature was raised from 25°C to 45°C, cells expressing both TRPV1 and Pirt exhibited significantly larger inward currents than cells expressing TRPV1 alone (3.2 ± 0.4 nA versus 1.6 ± 0.2 nA; $p = 0.0004$) (Figure 5A). We also examined whether coexpression of Pirt in these cells can increase TRPV1-mediated current activated by capsaicin. Consistent with the DRG neuron experiment, addition of Pirt significantly enhanced capsaicin-activating current only at higher concentrations (5 and 10 μM; Figure 5C). Again, the EC_{50} values of capsaicin for these two groups of HEK293 cells were not significantly different (0.78 ± 0.03 and 0.67 ± 0.04 μM for Pirt/TRPV1 and TRPV1 cells, respectively). The TRPV1 antagonist capsazepine completely inhibited capsaicin activation in HEK293 cells expressing both TRPV1 and Pirt, suggesting that the increased current is not due to activation of another channel (Figure S6). Furthermore, current-voltage relationships for capsaicin-evoked currents in HEK293 cells coexpressing TRPV1 and Pirt showed a relationship characteristic of TRPV1 (Figures S6B–S6D). The total protein levels and cell-surface expression of TRPV1 in HEK293 cells were not altered by coexpression of Pirt (Figure 5D). Together, these results indicate that Pirt alone is sufficient to enhance TRPV1-mediated currents in the absence of any other DRG-specific proteins.

Besides TRPV1, we also tested whether Pirt can modulate TRPA1-mediated current. We transfected Pirt cDNA into TRPA1 stably expressing HEK293 cells (Hill and Schaefer, 2007) and measured mustard oil-evoked currents. Unlike the TRPV1 experiments, expression of Pirt has no effect on TRPA1-mediated current (Figure 5E).

Pirt Binds to TRPV1

Pirt positively regulates TRPV1 activity, raising the possibility that TRPV1 and Pirt may form a complex. To address this possibility, we tested whether Pirt can coimmunoprecipitate TRPV1 when both proteins are expressed in HEK293 cells. When cell lysates of HEK293 cells transfected with TRPV1 and Pirt-myc were immunoprecipitated with anti-myc antibody, TRPV1 was specifically precipitated in the coexpressing cells (Figure 6A). We also examined binding of Pirt-myc to other TRPs. Interestingly, Pirt could bind TRPM8 but not TRPA1 (Figure 6A).

To determine the TRPV1-binding site in the intracellular regions of Pirt, we made GST fusion constructs, which include sequences encoding the N- (first 53 amino acids of Pirt; GST-N) or C-terminal (last 26 amino acids of Pirt; GST-C) region of Pirt. The constructs were individually transfected with TRPV1 into HEK293 cells and the GST pull-down assay was performed to study the protein-protein interaction. The C terminus of Pirt binds strongly to TRPV1, whereas

NIH-PA Author Manuscript

NIH-PA Author Manuscript

NIH-PA Author Manuscript

the N terminus binds weakly and GST alone does not bind (Figure 6B). Again, the C terminus binds TRPM8 (Figure 6B). However, Pirt fails to bind GluR1, a subunit of the AMPA-responsive class of glutamate receptors (Figure 6B). These results support the idea that Pirt interacts with specific TRPs.

Pirt Binds to Phosphoinositides

Since the C terminus of Pirt contains a cluster of positively charged residues (Figure 1A), a characteristic of PIP-binding domains, we examined the interaction between these two molecules using PIP_2-conjugated agarose beads in protein pull-down experiments. GST-C bound to the PIP_2 beads, (Figure 6C), while GST-N or GST alone did not interact with PIP_2 beads. We further tested whether Pirt binds other PIPs using PIP strips, nitrocellulose membranes containing various immobilized PIPs.

We found that the GST-C, but not GST alone, bound most PIPs, whereas no or weak interaction was detected with control phospholipids or blank areas (Figure 6D). To study the binding of Pirt and PIPs in a more physiological context (i.e., a bilayer), we performed a liposomal binding assay on a series of liposomal preparations containing different PIPs. The purified GST-C showed strong association with PIP_2- and PIP_3-containing liposomes but weak binding to phosphatidylinositide (PI)-containing liposome or control liposome composed of phosphatidylserine (PS) and phosphatidylcholine (PC) only (Figure 6E). Similar results were obtained using cytosolic fractions of HEK293 cells expressing GST-C (data not shown). GST alone did not show strong binding to these liposomes. The data from these different approaches clearly show that Pirt is a PIP-binding protein and it binds various PIPs, including PIP_2, but not PI and other negative controls.

Since the regulation of TRPV1 by PIP_2 is well documented in the literature, we focused our subsequent analysis on $PI(4,5)P_2$. To determine whether Pirt binding to PIP_2 is dependent on the cluster of basic residues in the C terminus, we generated two mutant forms of GST-Pirt C-terminal fusion protein. In one mutated protein (GST-C-3Q, Figure 7A), three lysines were changed to three glutamines, whereas the second mutant (GST-C-6A, Figure 7A) had five lysines and one arginine mutated to six alanines. As predicted, both mutated C termini failed to bind PIP_2 beads, suggesting that these positively charged residues are necessary for PIP_2 binding (Figure 7B). Surprisingly, both mutated fusion proteins retained the ability to bind TRPV1 (Figure 7C).

Pirt and PIP_2 Require Each Other to Enhance TRPV1

Since the C terminus of Pirt can bind both TRPV1 and PIP_2, we tested whether the C terminus alone is sufficient to modulate TRPV1 activity. Strikingly, when GST-C was expressed in TRPV1 stably expressing HEK293 cells, it significantly enhanced heat-evoked current as compared to control cells expressing GST alone (Figure 6F). However, when the mutated C terminus of GST-C-3Q was expressed in TRPV1 stably expressing cells, it showed heat-evoked current identical to cells expressing GST alone (Figure 7D; compare to Figure 6F). Together these data suggest that the basic residues in the last 26 amino acids of Pirt are crucial for PIPs' binding and Pirt function.

Since several studies have indicated that PIP_2 enhances TRPV1 activity, it is important to determine if the positive effects of PIP_2 on TRPV1 are dependent on Pirt (Liu et al., 2005; Stein et al., 2006; Lukacs et al., 2007). We added 10 μM PIP_2-diC8 to the patch pipette solution and recorded whole-cell capsaicin-evoked currents in WT and $Pirt^{-/-}$ DRG neurons. In parallel, we used 10 μM PI-diC8 in the pipette solution as a negative control. Recent studies have shown that PI does not have a strong effect on TRPV1 activity (<10% of that of PIP_2; Lukacs et al., 2007) and does not interfere with the association between TRPV1 and CaM (Kwon et al.,

NIH-PA Author Manuscript

NIH-PA Author Manuscript

NIH-PA Author Manuscript

2007). Furthermore, our data showed that Pirt does not bind to PI (Figure 6D). In WT neurons, PIP_2 strongly enhanced capsaicin-induced currents, as compared to PI controls. Importantly, PIP_2 had no effect on capsaicin–evoked currents in *Pirt*$^{-/-}$ neurons (Figure 7E). Thus, the potentiation of TRPV1 activity by PIP_2 requires Pirt.

PIP_2 has also been shown to have an inhibitory effect on TRPV1, particularly at a low stimulus strength (Chuang et al., 2001; Lukacs et al., 2007). A site (42 amino acids) within the C terminus of TRPV1 was found to be required for PIP_2-mediated inhibition (Prescott and Julius, 2003). A mutant form of TRPV1 without this site exhibited stronger current than WT TRPV1 and failed to be potentiated by PLC-coupled receptor activation as observed for the WT channel. These data suggest that this is the only site required for the PIP_2 inhibitory effect. To determine whether Pirt plays a role in PIP_2 inhibitory effect, we tested the ability of Pirt to modulate mutant TRPV1 (TRPV1D42)-mediated current. When 0.1 μM capsaicin was applied, significantly stronger currents were found in HEK293 cells expressing TRPV1Δ42 than those found in cells expressing WT TRPV1, confirming the previous finding. Strikingly, coexpression of Pirt further enhances TRPV1Δ42-mediated current (Figure 7F). Again, at this low level of capsaicin, Pirt has no significant effect on WT TRPV1-mediated current. Furthermore, Pirt can still bind to TRPV1Δ42 in vitro, suggesting that another region of TRPV1 is required for binding Pirt (Figure S7). Together, these data indicate that Pirt is unlikely to be involved in the PIP_2-mediated inhibitory effect on TRPV1.

DISCUSSION

Phosphoinositides such as PIP_2 are emerging as important modulators of TRP channel activity. Here, we demonstrate that Pirt, a membrane protein, binds both PIP_2 and TRPV1 and positively regulates TRPV1 via PIP_2. Pirt is highly conserved among vertebrates, and no closely related invertebrate homologs were found by a genome-wide sequence search, suggesting that vertebrates have acquired additional regulatory subunits for TRP channels. The expression of Pirt is restricted to the PNS (predominantly DRG and trigeminal ganglia) and is not found in the central nervous system (CNS). Therefore, the modulation of TRPV1 activity by Pirt likely occurs in these peripheral neurons but not in higher-order neurons within the CNS. Since Pirt is also expressed in TRPV1-negative neurons in DRG, it may be involved in regulating other TRP channel activity.

Pirt$^{-/-}$ mice show noxious heat and capsaicin behavioral phenotypes that resemble, but are less severe than, those observed in *TRPV1*$^{-/-}$ mice. These data support the hypothesis that TRPV1 works as a primary sensor of noxious heat and capsaicin, while Pirt regulates TRPV1 activity. Pirt itself does not exhibit any channel activity upon noxious heat or capsaicin treatment (data not shown). Whole-cell recordings from DRG neurons and TRPV1 stably expressing HEK293 cells suggest that Pirt enhances TRPV1-mediated currents. This enhancement is not due to altered cell surface level expression of TRPV1 by Pirt based on our surface biotinylation data. Single-channel recording experiments should give us more detailed information on how Pirt affects conductance, open time, or open probability of TRPV1.

Consistent with a role for Pirt in potentiating TRPV1 sensation, we found that Pirt physically interacts with TRPV1. Therefore, it is likely that Pirt functions as a regulatory subunit of the TRPV1 complex. More importantly, the C terminus of Pirt alone can bind PIPs and TRPV1 and enhance heat-evoked current through TRPV1. The basic residues in the C terminus of Pirt are required for PIP_2 but not TRPV1 binding, suggesting that the 26 amino acids of the C terminus contain separate binding domains for PIP_2 and TRPV1. In addition, the mutant form of the Pirt C terminus failed to modulate TRPV1 function, indicating that PIP_2 binding is essential for Pirt regulation of TRPV1 and that the binding to TRPV1 alone is not sufficient to enhance the channel's activity. The C terminus of Pirt can bind to PIPs other than PIP_2 in

NIH-PA Author Manuscript

NIH-PA Author Manuscript

NIH-PA Author Manuscript

vitro, suggesting that nonspecific electrostatic interactions contribute strongly to the binding between the basic residues and the negatively charged inositides. Such interactions with PIPs are well characterized for several proteins, such as MARCKS, which contain clusters of positively charged residues (Wang et al., 2001). The broad PIP binding of Pirt is consistent with other findings that TRPV1 can be modulated by various PIPs besides PIP_2 (Kwon et al., 2007; Lukacs et al., 2007). Therefore, it is probable that other PIPs may also participate in Pirt's regulation of TRPV1.

It has been shown that PIP_2 has an inhibitory effect on heat- and capsaicin-evoked TRPV1 current (Chuang et al., 2001; Prescott and Julius, 2003). However, other studies have found that PIP_2 has an activating effect on TRPV1. For example, direct application of PIP_2 to the inner leaflet of TRPV1-expressing membranes led to channel activation, while sequestering PIP_2 with polylysine inhibited channel function (Stein et al., 2006). A more recent study may reconcile the discrepancy (Lukacs et al., 2007). These authors found that PIP_2 has a dual effect on TRPV1: inhibitory at low capsaicin concentrations and activating at high capsaicin concentrations. Our data support previous findings that PIP_2 can have both activating and inhibitory effects on TRPV1 and highlight the role of Pirt in mediating the activating effect of PIP_2.

Our PIP_2 application experiments suggest that PIP_2 has an activating effect on TRPV1 at high capsaicin concentrations (5 μM). Importantly, Pirt is required for this positive effect. Other groups have observed PIP_2 activating effects on TRPV1 activity in heterologous systems where Pirt is unlikely to be present (Stein et al., 2006; Lukacs et al., 2007). In these cases, the experiments were performed using inside-out recording with direct application of PIP_2 to the inner leaflets of membranes. Therefore, it is likely that the very high levels of PIP_2 applied in their experimental systems can bypass the requirement for Pirt. Furthermore, in our capsaicin dose-response experiments, the activating effect of Pirt on TRPV1-mediated currents was only prominent when high concentrations of capsaicin (5 and 10 μM) were applied. This effect is also PIP_2 dependent (Figure 7D). Therefore, both Pirt and PIPs are required for optimal TRPV1 function.

At low concentrations of capsaicin, PIP_2 plays an inhibitory role on TRPV1. It has been proposed that the inhibitory effect maybe indirect and that other PIP_2-binding protein(s) may be involved (Stein et al., 2006; Lukacs et al., 2007). Our data show that Pirt is not involved in this modulation since Pirt can further enhance the activity of TRPV1Δ42. Therefore, Pirt plays an essential role only in the activating effect of PIP_2 but not in its inhibitory effect. These results also indicate that the inhibitory effect of PIP_2 at low capsaicin concentration masks the activating effect of Pirt on TRPV1. However, removal of the inhibitory effect by bradykinin-activated PLC or deleting the last 42 amino acids of TRPV1 unmask the activating effect of Pirt. We have shown that PIP_2 modulates TRPV1 in two ways: inhibition by interacting with the last 42 amino acids of TRPV1 and activation via association with Pirt at a different region of TRPV1. Furthermore, hydro-lysis of PIP_2 by PLC may differ in these situations.

Our behavioral and cellular studies show that Pirt does not play a role in TRPA1 function, suggesting that Pirt does have specificity toward certain TRP channels. Interestingly, Pirt also fails to bind TRPA1. It will be interesting to test if the failure of Pirt to regulate TRPA1 is due to its inability to bind this channel. However, we cannot rule out the possibility that Pirt affects the activities of other TRPs, especially as PIP_2 has been implicated in the regulation of many TRP channels (Hardie, 2007; Voets and Nilius, 2007). For example, TRPM8, the cold and menthol sensor (Colburn et al., 2007; Dhaka et al., 2007), requires PIP_2 for activation (Rohacs et al., 2005). Interestingly, Pirt can also bind TRPM8. Therefore, Pirt may regulate the activities of other TRP channels via PIP_2. Because TRP channels play critical roles in nociception,

NIH-PA Author Manuscript

NIH-PA Author Manuscript

NIH-PA Author Manuscript

uncovering the interactions between Pirt, TRPs, and PIPs should provide a better understanding of pain transduction.

EXPERIMENTAL PROCEDURES

Molecular Biology—The arms of the *Pirt* targeting constructs were subcloned from a 129/SvJ genomic DNA lambda phage clone (Invitrogen) and ligated with an EGFPf-IRES-rtTA-CAN cassette. $Pirt^{+/-}$ mice were generated using the targeting construct by a transgenic mouse facility at the University of Cincinnati. Details of the generation of *Pirt* knockout mice are available in the Supplemental Data. The DNA fragments corresponding to the N- (1−53) and C- (110−135) terminal regions of Pirt were generated by PCR amplification of *Pirt* cDNA and cloned into pCMV-GST (Tsai and Reed, 1997) in frame with glutathione S-transferase (GST). The mutant forms of the Pirt C terminus were generated using a QuikChange Site-Directed Mutagenesis Kit (Stratagene).

In Situ Hybridization—Nonisotopic in situ hybridization on frozen sections from WT E14.5 embryos was performed as previously described using cRNA probes (Dong et al., 2001).

Anti-Pirt Serum—Rabbit polyclonal antibody was raised against a synthetic peptide, EVLPKALEVDERSPESKDL, corresponding to the N terminus of mouse Pirt by Protein-tech Group, Inc.

Cell Culture—DRG neurons were collected from all spinal levels from 3- to 4-week-old mice and then were dissociated and plated on coated glass coverslips. Cells were plated for 24 hr before use. TRPV1 and TRPA1 stably expressing HEK cells were obtained from Drs. M. Caterina (Johns Hopkins University) and N. Tigue (GlaxoSmithKline), respectively. For transient transfection of HEK293 cells, Lipofectamine (Invitrogen) was used. Details of Neuronal and HEK cell culture conditions and transfection are available (see Supplemental Data).

Coimmunoprecipitation—HEK293 cells were transfected with a Pirt-myc fusion construct along with a TRPV1, TRPM8, or TRPA1 plasmid. After 24 hr, cell lysates were collected and supernatant was extracted. Myc antibody was added to the supernatant and incubated overnight. Gammabind Plus Sepharose beads (GE Healthcare Life Sciences) were added to the lysates, and the mixtures were incubated for an additional 3 hr and the proteins were eluted using 2× SDS-PAGE sample buffer (see Supplemental Data).

GST Pull Down—The GST-N, GST-C fusion, and GST constructs were separately transfected with various ion channel genes into HEK293 cells. After 24 hr, cell lysates were incubated using glutathione-agarose beads. Specifically bound proteins were eluted from the beads using 2× protein sample buffer. Details are available (see Supplemental Data).

Biotinylation of Cell-Surface Proteins—TRPV1 stably expressing HEK293 cells were transfected with Pirt-containing plasmid. After 24 hr, the HEK cells or cultured DRG neurons were then incubated with 1.0 mg/ml sulfo-NHS-SS-Biotin (Pierce) in PBS for 30 min at 4°C. After quenching, cells were lysed in 500 μl of RIPA buffer. Supernatant from cell lysate was added to BSA-Blocked ultralink-neutravidin beads (Pierce) and incubated for 2 hr. The proteins were eluted from the beads using 2× SDS-PAGE sample buffer and western blot was performed using the anti-TRPV1 antibody (from Dr. M. Caterina). Details are available (see Supplemental Data).

PIP_2 Bead Binding and PIP Strips—HEK293 cells were singly transfected with GST-N, GST-C, or GST. The cells were lysed and spun down at 10,000 × g for 10 min. The supernatants

NIH-PA Author Manuscript

NIH-PA Author Manuscript

NIH-PA Author Manuscript

were added to the PIP beads or PIP strips (Echelon Biosciences). Details are available (see Supplemental Data).

Liposomal Binding Assay—Liposomes were prepared by mixing PC, PS, and PIPs at the proportions of 49.5%, 49.5%, and 1.0%, respectively, drying the mixture under vacuum, and resuspending to a final concentration of 1 mg/ml of total phospholipid in a buffer composed of HEPES (50 mM), NaCl (100 mM), and EDTA (0.5 mM). After sonicating for 30 min, liposomes were collected by centrifugation at 16,000 × g for 10 min and resuspended in binding buffer. Fifty microliters of liposome suspension was mixed with 0.1 μg of purified protein and incubated at room temperature for 15 min. Liposomes were pelleted at 16,000 × g for 10 min and bound fraction was analyzed by western blot (see Supplemental Data).

Behavioral Assays—Behavioral tests were performed by individuals blind to genotype. The mice used in the tests were backcrossed to C57Bl/6 mice for at least five generations and were 2- to 3 month-old (20−30 g) males. All experiments were performed under protocol approved by the Animal Care and Use Committee of Johns Hopkins University School of Medicine. Details for all the behavior assays are available in the Supplemental Data.

Electrophysiology—Whole-cell voltage-clamp recordings were performed. For neurons, only small neurons were selected for recording. For HEK293 cells, transfected cells were identified by GFP fluorescence. Only one neuron or one HEK cell was tested per coverslip.

Capsaicin, mustard oil, and GABA were used as agonists to TRPV1, TRPA1, and GABA receptors, respectively. When examining heat-evoked current responses, a preheated solution was used to increase bath temperature; the heating was an in-line solution heater and used the TC-324B temperature controller (Warner Instruments). Statistical comparisons were made using un-paired Student's t test and differences were considered significant at $p < 0.05$. Details are available in the Supplemental Data.

Supplementary Material

Refer to Web version on PubMed Central for supplementary material.

ACKNOWLEDGMENTS

We thank Drs. M. Caterina for TRPV1 stable HEK293 cells, TRPV1, and TRPM8 cDNAs; P. Worley for GluR1-HA cDNA and pCMV-GST construct; N. Tigue for hTRPA1 stable HEK293 cells. We also thank Drs. M. Caterina, M. Chung, and A. Kolodkin for helpful comments on the manuscript. The cloning of *Pirt* and initial in situ hybridization using *Pirt* cRNA were carried out in the laboratory of Dr. D. Anderson (California Institute of Technology). The liposomal pulldown experiment was performed in the laboratory of Dr. S.H. Snyder (Johns Hopkins University). X.D. is supported by an NINDS grant (NS054791).

REFERENCES

Bautista DM, Jordt SE, Nikai T, Tsuruda PR, Read AJ, Poblete J, Yamoah EN, Basbaum AI, Julius D. TRPA1 mediates the inflammatory actions of environmental irritants and proalgesic agents. Cell 2006;124:1269–1282. [PubMed: 16564016]

Caterina MJ, Julius D. Sense and specificity: a molecular identity for nociceptors. Curr. Opin. Neurobiol 1999;9:525–530. [PubMed: 10508737]

Caterina MJ, Schumacher MA, Tominaga M, Rosen TA, Levine JD, Julius D. The capsaicin receptor: A heat-activated ion channel in the pain pathway. Nature 1997;389:816–824. [PubMed: 9349813]

Caterina MJ, Leffler A, Malmberg AB, Martin WJ, Trafton J, Petersen-Zeitz KR, Koltzenburg M, Basbaum AI, Julius D. Impaired nociception and pain sensation in mice lacking the capsaicin receptor. Science 2000;288:306–313. [PubMed: 10764638]

NIH-PA Author Manuscript

NIH-PA Author Manuscript

NIH-PA Author Manuscript

Chuang HH, Prescott ED, Kong H, Shields S, Jordt SE, Basbaum AI, Chao MV, Julius D. Bradykinin and nerve growth factor release the capsaicin receptor from PtdIns(4,5)P2-mediated inhibition. Nature 2001;411:957–962. [PubMed: 11418861]

Colburn RW, Lubin ML, Stone DJ Jr. Wang Y, Lawrence D, D'Andrea MR, Brandt MR, Liu Y, Flores CM, Qin N. Attenuated cold sensitivity in TRPM8 null mice. Neuron 2007;54:379–386. [PubMed: 17481392]

Davis JB, Gray J, Gunthorpe MJ, Hatcher JP, Davey PT, Overend P, Harries MH, Latcham J, Clapham C, Atkinson K, et al. Vanilloid receptor-1 is essential for inflammatory thermal hyperalgesia. Nature 2000;405:183–187. [PubMed: 10821274]

Dhaka A, Murray AN, Mathur J, Earley TJ, Petrus MJ, Patapoutian A. TRPM8 is required for cold sensation in mice. Neuron 2007;54:371–378. [PubMed: 17481391]

Dong X, Han S, Zylka MJ, Simon MI, Anderson DJ. A diverse family of GPCRs expressed in specific subsets of nociceptive sensory neurons. Cell 2001;106:619–632. [PubMed: 11551509]

Guler AD, Lee H, Iida T, Shimizu I, Tominaga M, Caterina M. Heat-evoked activation of the ion channel, TRPV4. J. Neurosci 2002;22:6408–6414. [PubMed: 12151520]

Hardie RC. TRP channels and lipids: from Drosophila to mammalian physiology. J. Physiol 2007;578:9–24. [PubMed: 16990401]

Hill K, Schaefer M. TRPA1 is differentially modulated by the amphipathic molecules trinitrophenol and chlorpromazine. J. Biol. Chem 2007;282:7145–7153. [PubMed: 17218316]

Huang J, Zhang X, McNaughton PA. Modulation of temperature-sensitive TRP channels. Semin. Cell Dev. Biol 2006;17:638–645. [PubMed: 17185012]

Kwan KY, Allchorne AJ, Vollrath MA, Christensen AP, Zhang DS, Woolf CJ, Corey DP. TRPA1 contributes to cold, mechanical, and chemical nociception but is not essential for hair-cell transduction. Neuron 2006;50:277–289. [PubMed: 16630838]

Kwon Y, Hofmann T, Montell C. Integration of phosphoinosi-tide- and calmodulin-mediated regulation of TRPC6. Mol. Cell 2007;25:491–503. [PubMed: 17317623]

Liu B, Zhang C, Qin F. Functional recovery from desensitization of vanilloid receptor TRPV1 requires resynthesis of phosphatidylinositol 4,5-bisphosphate. J. Neurosci 2005;25:4835–4843. [PubMed: 15888659]

Lo L, Dormand E, Greenwood A, Anderson DJ. Comparison of the generic neuronal differentiation and neuron subtype specification functions of mammalian achaete-scute and atonal homologs in cultured neural progenitor cells. Development 2002;129:1553–1567. [PubMed: 11923194]

Lukacs V, Thyagarajan B, Varnai P, Balla A, Balla T, Rohacs T. Dual regulation of TRPV1 by phosphoinositides. J. Neurosci 2007;27:7070–7080. [PubMed: 17596456]

Montell C. The TRP superfamily of cation channels. Sci. STKE 2005;2005:272.

Prescott ED, Julius D. A modular PIP2 binding site as a determinant of capsaicin receptor sensitivity. Science 2003;300:1284–1288. [PubMed: 12764195]

Rohacs T, Lopes CM, Michailidis I, Logothetis DE. PI(4,5)P2 regulates the activation and desensitization of TRPM8 channels through the TRP domain. Nat. Neurosci 2005;8:626–634. [PubMed: 15852009]

Scott, SA. Sensory neurons: Diversity, development and plasticity. Oxford University Press; Oxford: 1992.

Stein AT, Ufret-Vincenty CA, Hua L, Santana LF, Gordon SE. Phosphoinositide 3-kinase binds to TRPV1 and mediates NGF-stimulated TRPV1 trafficking to the plasma membrane. J. Gen. Physiol 2006;128:509–522. [PubMed: 17074976]

Tjolsen A, Berge OG, Hunskaar S, Rosland JH, Hole K. The formalin test: an evaluation of the method. Pain 1992;51:5–17. [PubMed: 1454405]

Tominaga M, Caterina MJ, Malmberg A, Rosen TA, Gilbert H, Skinner K, Raumann B, Basbaum AI, Julius D. The cloned capsaicin receptor integrates multiple pain-producing stimuli. Neuron 1998;21:531–543. [PubMed: 9768840]

Tsai RYL, Reed RR. Using a eukaryotic GST fusion vector for proteins difficult to express in E. coli. Biotechniques 1997;23:794–798. [PubMed: 9383538]

Voets T, Nilius B. Modulation of TRPs by PIPs. J. Physiol 2007;582:939–944. [PubMed: 17395625]

Wang J, Arbuzova A, Hangyas-Mihalyne G, McLaughlin S. The effector domain of myristoylated alanine-rich C kinase substrate binds strongly to phosphatidylinositol 4,5-bisphosphate. J. Biol. Chem 2001;276:5012–5019. [PubMed: 11053422]

NIH-PA Author Manuscript

NIH-PA Author Manuscript

NIH-PA Author Manuscript

NIH-PA Author Manuscript

NIH-PA Author Manuscript

NIH-PA Author Manuscript

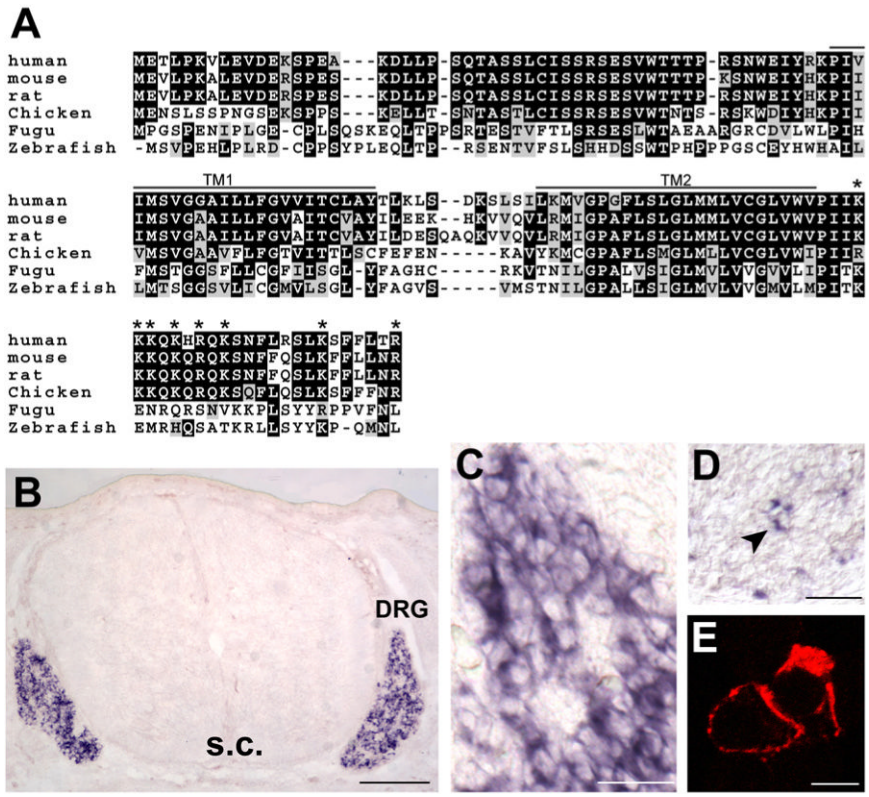

Figure 1. *Pirt* Encodes a Two Transmembrane Domain Protein and Is Expressed Predominantly in DRG

(A) Alignment of amino acid sequences of Pirt from various vertebrates. Residues shaded in black are identical in >50% of the predicted proteins; similar residues are highlighted in gray. The predicted transmembrane domains (TM1 and TM2) and positively charged residues in the C-terminal region (asterisk) are indicated. (B–D) In situ hybridization with cRNA probes detecting *Pirt*. (B) Cross-section through the trunk region of E14.5 mouse embryo. Strong *Pirt* signal was present in DRG but absent in the spinal cord (s.c.). (C) A higher magnification view of the DRG region. (D) Cross-section of sympathetic ganglia from E14.5 embryo. A small subset of neurons was stained (arrowhead). (E) Membrane localization of Pirt. Pirt cDNA was tagged with a myc epitope at the C terminus of the protein and expressed in PC12 cells. When the plasma membrane was permeabilized by detergent, membrane localization of the Pirt-myc fusion protein was observed by anti-myc antibody staining (two adjacent cells shown). Under nondetergent conditions no specific staining was found (data not shown). Similar results were obtained using an antibody against the N-terminus of Pirt (data not shown). Scale bars in (B), (C), (D), and (E) represent 100, 50, 40, and 10 μm, respectively.

NIH-PA Author Manuscript

NIH-PA Author Manuscript

NIH-PA Author Manuscript

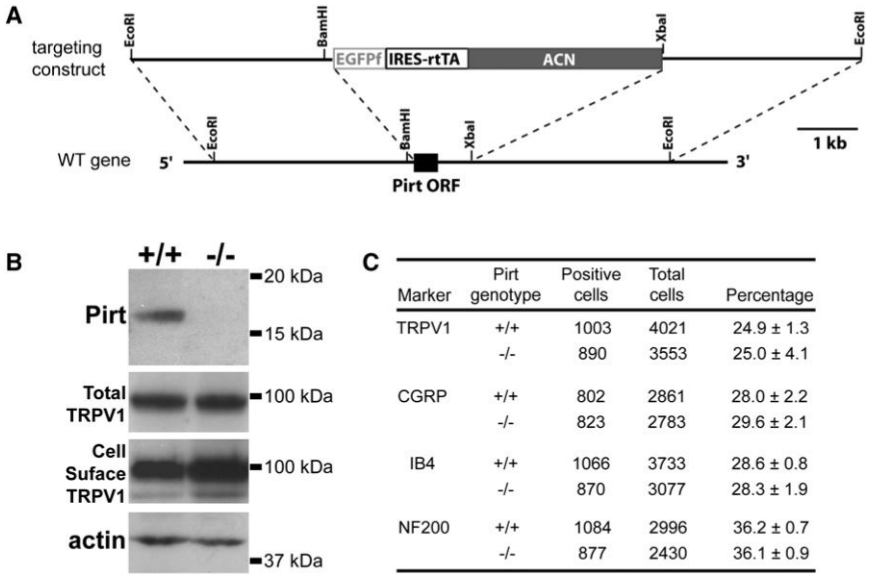

C

Marker	Pirt genotype	Positive cells	Total cells	Percentage
TRPV1	+/+	1003	4021	24.9 ± 1.3
	-/-	890	3553	25.0 ± 4.1
CGRP	+/+	802	2861	28.0 ± 2.2
	-/-	823	2783	29.6 ± 2.1
IB4	+/+	1066	3733	28.6 ± 0.8
	-/-	870	3077	28.3 ± 1.9
NF200	+/+	1084	2996	36.2 ± 0.7
	-/-	877	2430	36.1 ± 0.9

Figure 2. Generation of *Pirt* Null Mice

(A) Targeting strategy for disrupting the *Pirt* gene. The entire ORF of *Pirt* (black box) was replaced by farnesylated enhanced GFP (EGFPf) followed by IRES-reverse-tetracycline-transactivator (IRES-rtTA). ACN is a self-excising neomycin expression cassette. (B) Western blots of DRG lysates derived from $Pirt^{+/+}$ and $Pirt^{-/-}$ mice using antibodies specifically against Pirt, TRPV1, and β-actin demonstrate that Pirt protein is specifically deleted in $Pirt^{-/-}$ mice. TRPV1 expression in cultured DRG neurons was measured by western blot after plasma membrane proteins were biotinylated and purified with streptavidin. The molecular weights are indicated on the right. (C) Immunofluorescence staining of DRG sections show normal proportions of TRPV1-, CGRP-, IB4-, and NF200-expressing neurons in $Pirt^{-/-}$ mice (n = 3). The total number of DRG neurons was determined by costaining with the pan-neuronal marker NeuN (Lo et al., 2002). Values are mean ± standard error.

NIH-PA Author Manuscript

NIH-PA Author Manuscript

NIH-PA Author Manuscript

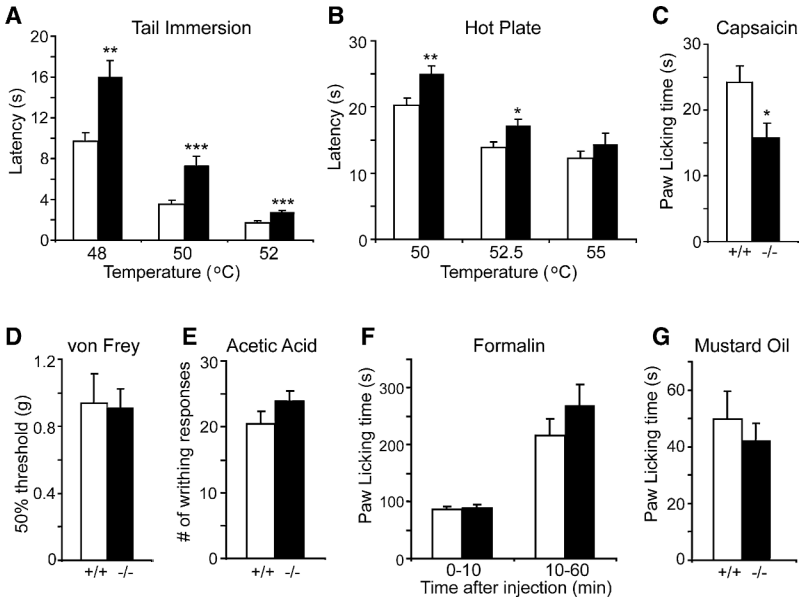

Figure 3. *Pirt*$^{-/-}$ Mice Show Impaired Behavioral Responses to Noxious Heat and Capsaicin

(A) Tail-withdrawal latency of *Pirt*$^{-/-}$ mice (black bars) in the tail immersion test was significantly increased as compared with *Pirt*$^{+/+}$ mice (white bars) when water bath temperature was at 48°C (*Pirt*$^{+/+}$: n = 15; *Pirt*$^{-/-}$: n = 16), 50°C (+/+: n = 21; −/−: n = 21), and 52°C (+/+: n = 9; −/−: n = 10). (B) Paw-withdrawal latency of *Pirt*$^{-/-}$ mice on hot plate was significantly longer than in WT mice at 5C (+/+: n = 21; −/−: n = 22) and 52.5°C (+/+: n = 15; −/−: n = 17) but not at 55°C (+/+: n = 11; −/−: n = 14). (C) Behavioral responses to intraplantar injection of capsaicin (0.6 μg) were measured for *Pirt*$^{+/+}$ (n = 18) and *Pirt*$^{-/-}$ (n = 18) mice for 10 min after injection. (D) Responsiveness to mechanical stimulation as measured by von Frey test was the same in WT (n = 8) and mutant (n = 9) mice. (E) *Pirt*$^{-/-}$ mice (n = 18) showed a similar number of writhes in response to intraperitoneal acetic acid injection compared with WT mice (n = 16). (F) Paw licking times during phase I (0−10 min) and phase II (10−60 min) of the nociceptive response to formalin injection (Tjolsen et al., 1992) were not significantly different between the two genotypes (n = 14/genotype). (G) Behavioral responses to intraplantar injection of mustard oil (6 μl of 2.0%) were measured for *Pirt*$^{+/+}$ and *Pirt*$^{-/-}$ mice (n = 13/genotype) for 10 min after injection. *p < 0.05; **p < 0.01; ***p < 0.001 for *Pirt*$^{+/+}$ versus *Pirt*$^{-/-}$; two-tailed unpaired t test. All error bars represent standard error of the mean (SEM).

NIH-PA Author Manuscript

NIH-PA Author Manuscript

NIH-PA Author Manuscript

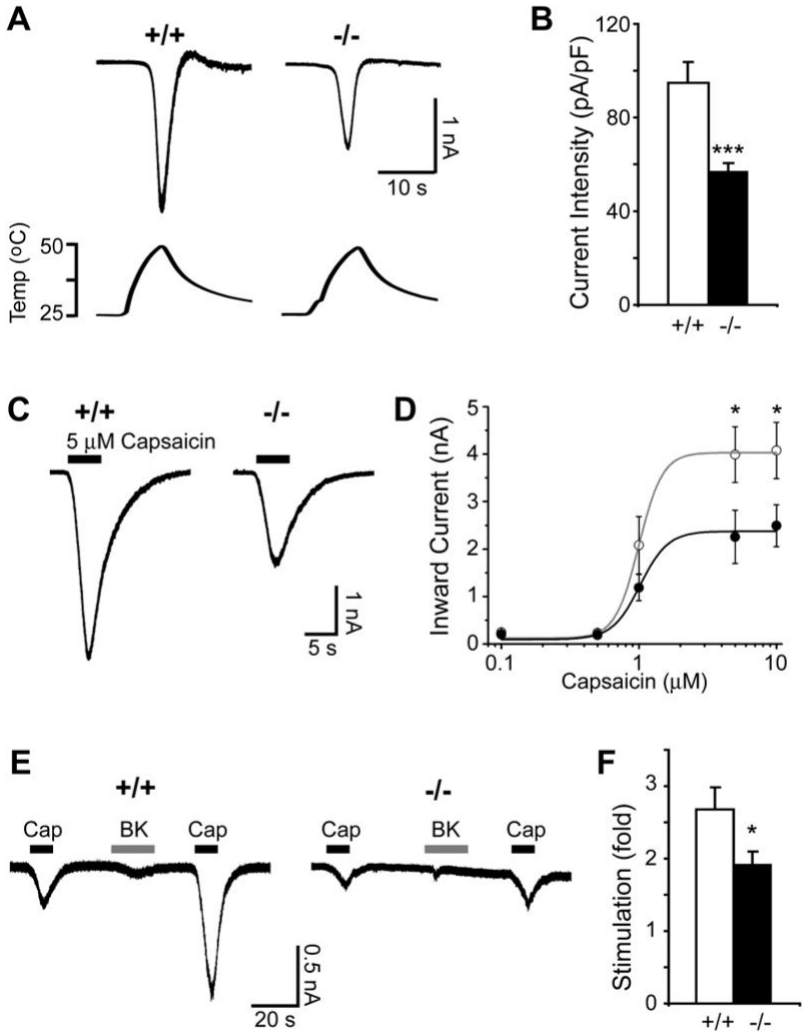

Figure 4. Heat- and Capsaicin-Evoked Currents Were Reduced in Pirt-Deficient DRG Neurons

(A) Responses of DRG neurons from $Pirt^{+/+}$ (+/+) and $Pirt^{-/-}$ (−/−) mice to heat. Current trace and temperature ramp (25°C –50°C) are shown on the top and bottom, respectively. (B) Current intensities of DRG neuron response to heat. Current intensities of WT (open bar, n = 39) and $Pirt^{-/-}$ (black bar, n = 33) neurons were significantly different (***$p < 0.005$). (C) Inward current response to application of 5 μM capsaicin (black line) in DRG neurons from $Pirt^{+/+}$ (+/+) and $Pirt^{-/-}$ (−/−) mice. (D) The concentration-response relationship expressed as inward current versus concentration of capsaicin in WT (open circles) and $Pirt^{-/-}$ (closed circles) neurons. Data points were fitted to the Hill equation. When 5 μM and 10 μM capsaicin were applied to DRG culture neurons of WT (n = 26 in 5 μM, n = 25 in 10 μM) and $Pirt^{-/-}$ (n = 26 at 5 μM, n = 20 at 10 μM) mice, respectively, the current sizes (*$p < 0.05$) and current intensities (data not shown) were significantly different. (E) Representative current traces from $Pirt^{+/+}$ (n = 15) and $Pirt^{-/-}$ (n = 16) neurons stimulated with capsaicin (0.1 μM, black line) followed by bradykinin (1 μM, gray line) and capsaicin (0.1 μM) again. (F) Potentiation by bradykinin was calculated by dividing post-treatment capsaicin-evoked currents by pre-treatment values. Wild-type neurons showed stronger potentiation by bradykinin than $Pirt^{-/-}$ neurons ($p = 0.041$). All error bars represent SEM.

NIH-PA Author Manuscript

NIH-PA Author Manuscript

NIH-PA Author Manuscript

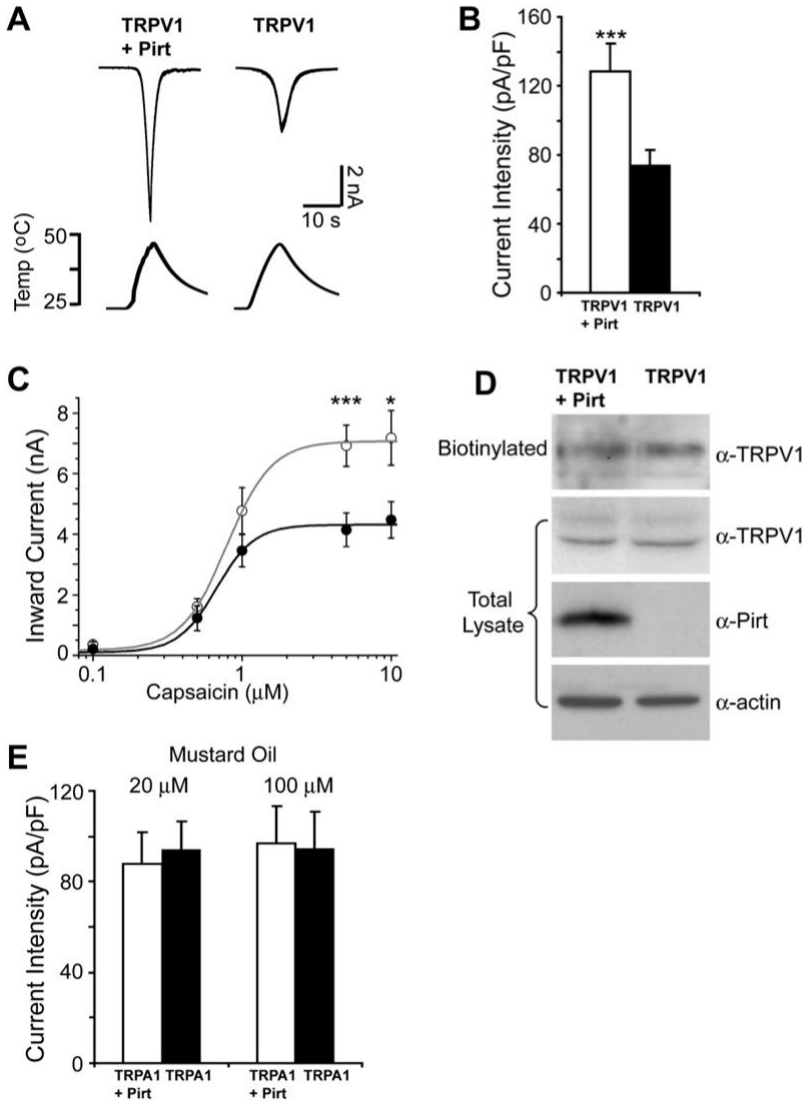

Figure 5. TRPV1-Mediated Currents Are Enhanced by Expression of Pirt

(A) Heat-evoked current traces in TRPV1 stably expressing HEK293 cells. Top shows current traces in TRPV1 cells cotransfected with Pirt and GFP (TRPV1 + Pirt) and TRPV1 cells transfected with GFP alone (TRPV1); bottom shows the ramp of heated buffer application. (B) Heat-evoked current intensities of TRPV1 cells expressing Pirt (open bar, n = 30) or TRPV1 alone (black bar, n = 30). Pirt significantly increases TRPV1 current in response to heat stimulation (***$p < 0.005$). (C) Capsaicin dose-response curves of TRPV1 stably expressing cells cotransfected with Pirt and GFP (open circles) and TRPV1 cells transfected with GFP alone (closed circles). When 5 μM and 10 μM capsaicin were applied to TRPV1/Pirt cells (n = 26 at 5 μM, n = 16 at 10 μM) and TRPV1 cells (n = 26 at 5 μM, n = 15 at 10 μM), respectively, the current sizes and current intensities (data not shown) indicated significantly different responses. Holding potential = −60 mV. (D) The expression level of TRPV1 in the TRPV1 stable HEK293 cells was measured by western blot after plasma membrane proteins were biotinylated and purified with streptavidin. β-actin was used as a loading control. (E) Mustard oil-evoked current intensities in TRPA1 stably expressing HEK293 cells. Twenty and one hundred micromolars of mustard oil were used to stimulate the cells. The current intensities of

TRPA1 cells expressing Pirt (open bar, n = 12) and TRPA1 alone (black bar, n = 12) were almost identical at both concentrations. All error bars represent SEM.

NIH-PA Author Manuscript
NIH-PA Author Manuscript
NIH-PA Author Manuscript

NIH-PA Author Manuscript
NIH-PA Author Manuscript
NIH-PA Author Manuscript

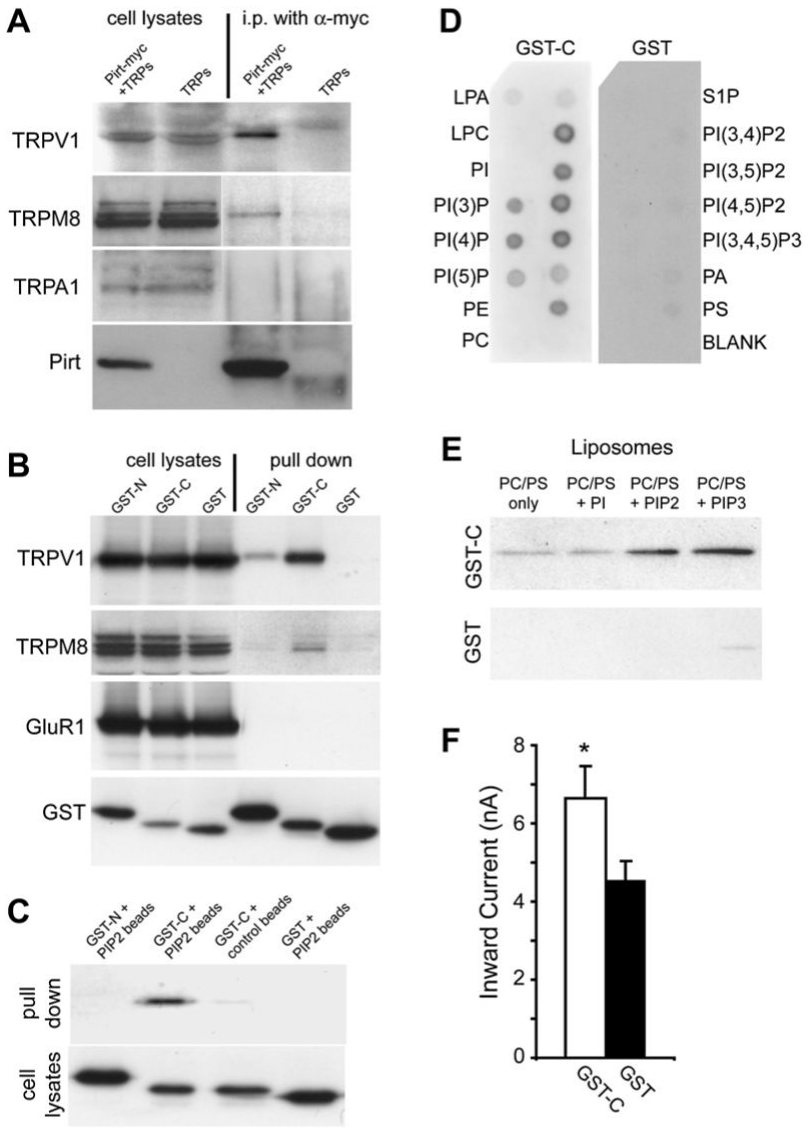

Figure 6. Pirt Binds to TRPV1 and PIPs

(A) Coimmunoprecipitation of TRP channels and Pirt in HEK293 cells. HEK293 cells transfected with different TRPs and Pirt-myc were immunoprecipitated with anti-myc antibody. Immunoprecipitates were detected by antibodies against corresponding TRPs and Pirt. The immunoblots of TRPs and Pirt in cell lysates indicate their expression levels before immunoprecipitation. Pirt forms a complex with TRPV1 and TRPM8 but not TRPA1. (B) GST pull-down assay of HEK293 cell lysates coexpressing TRPV1 with GST-N, GST-C, or GST alone and visualized by western blot analysis with anti-TRPV1 antibody. GST pull down of HEK293 cell lysates coexpressing either TRPM8 or HA-tagged GluR1 with GST-N, GST-C, and GST alone and visualized by western blot analysis with anti-TRPM8 or anti-HA antibodies, respectively. (C) GST-C binds PIP_2-conjugated agarose beads. PIP_2-conjugated agarose beads were used to pull down GST-N, GST-C, and GST from HEK293 cell lysates expressing these proteins. Control beads without PIP_2 were also used to pull down GST-C. (D) Protein-lipid overlays. Cell lysates from GST-C fusion protein comprised of the Pirt C terminus (left panel) or GST only (right panel) transfected HEK293 cells were used to probe PIP strips. For each strip, lipids were deposited in two rows and only labeled outside. The proteins were detected

NIH-PA Author Manuscript

NIH-PA Author Manuscript

NIH-PA Author Manuscript

by ECL after probing with anti-GST antibodies. Strong binding of GST-C to PIPs, PIP_2, and PIP_3 was observed but no binding was found with control lipids such as phosphatidylinositol (PI) and phosphatidylethanolamine (PE). (E) Liposomal pulldown assay. Liposomes composed of phosphatidylcholine (PC), phosphatidylserine (PS), and different PIPs were prepared as indicated in Experimental Procedures. PI-, PIP_2-, or PIP_3-containing or control (composed of PC and PS only) liposomes were incubated with the same amount (0.1 μg) of purified GST-C or GST and pelleted by centrifugation. Associated proteins were visualized by western blot with anti-GST antibody. (F) Heat-evoked current sizes of TRPV1 cells expressing GST-C (open bar, n = 29) or GST alone (black bar, n = 33). The C terminus of Pirt can significantly increase TRPV1 current response to heat stimulation (*$p < 0.05$). All error bars represent SEM.

NIH-PA Author Manuscript

NIH-PA Author Manuscript

NIH-PA Author Manuscript

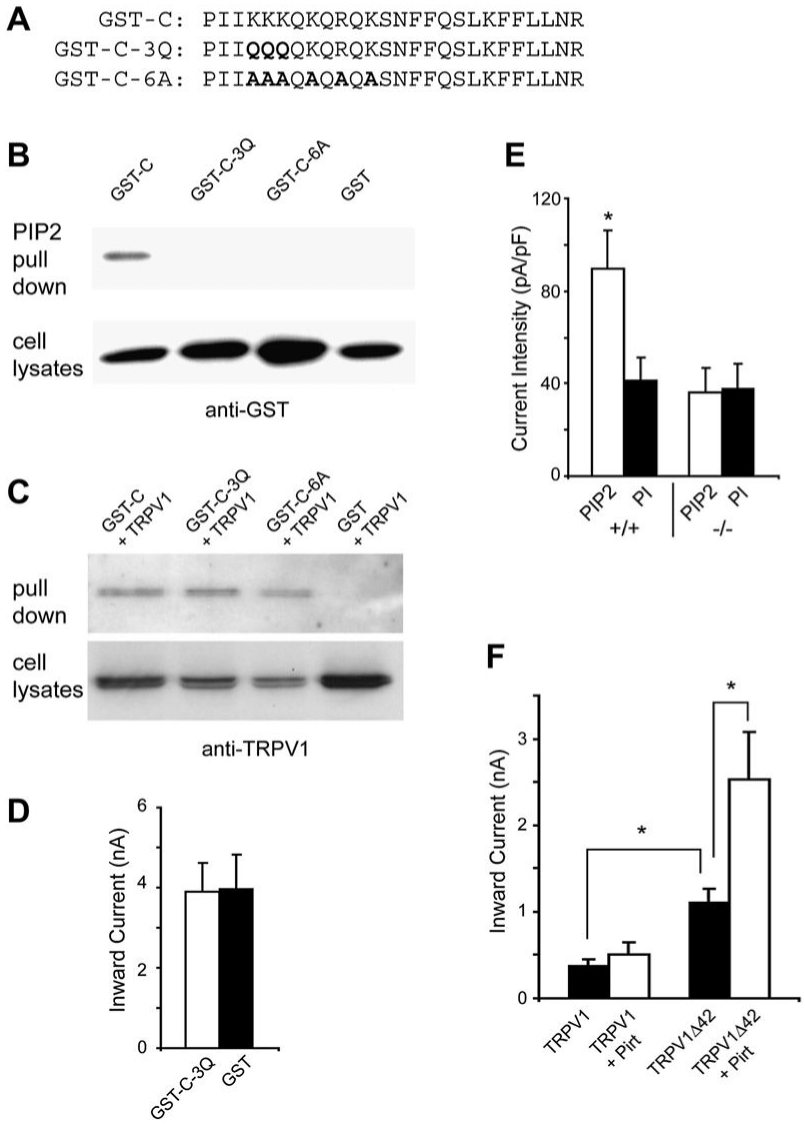

Figure 7. Pirt and PIP_2 Are Dependent on Each Other to Enhance TRPV1 Activity

(A) Sequences of WT and mutant forms of the Pirt C terminus, which were fused with GST. Bold letters indicate the mutated basic residues. (B) PIP_2-conjugated agarose beads failed to pull down GST-C-3Q and GST-C-6A from HEK293 cell lysates expressing these proteins. The pull-down products were immunoblotted by antibody against GST. (C) Binding of TRPV1 with GST-C-3Q or GST-C-6A in HEK293 cells. HEK293 cells transfected with TRPV1 and either GST-C, GST-C-3Q, or GST-C-6A were pulled down with glutathione-agarose beads. Immunoprecipitates were immunoblotted by anti-TRPV1 antibody. The mutant C termini still formed a complex with TRPV1. (D) Heat-evoked current sizes of TRPV1 stably expressing cells expressing GST-C-3Q (open bar, n = 18) or GST alone (black bar, n = 18). The mutant C terminus has no effect on TRPV1 activity. (E) Current densities of DRG neurons from $Pirt^{+/+}$ (+/+) and $Pirt^{-/-}$ (−/−) mice in response to 5 μM capsaicin. Whole-cell recordings were performed with either water-soluble PIP_2-diC8 (10 μM; Echelon Biosciences; open bars) or PI-diC8 (10 μM; black bar) added to the pipette solution. In WT neurons, PIP_2 (n = 27) significantly enhanced TRPV1-mediated current as compared to PI (n = 25; p = 0.017). In $Pirt^{-/-}$ neurons, PIP_2 (n = 25) did not show any effect on TRPV1 current as compared to PI (n = 19). (F) Currents of HEK293 cells transfected with WT TRPV1 or TRPV1Δ42 in the presence

NIH-PA Author Manuscript

NIH-PA Author Manuscript

NIH-PA Author Manuscript

or absence of Pirt in response to 0.1 μM capsaicin. Cells expressing TRPV1Δ42 alone (n = 9) showed significantly stronger current than those expressing WT channels (n = 11). Coexpressing Pirt can significantly potentiate TRPV1Δ42- (n = 10) but not WT TRPV1- (n = 12) mediated currents (*$p < 0.05$). All error bars represent SEM.